Optimizing OPC data sampling based on "orthogonal vector space"

Yuyang Sun*, Yee Mei Foong, Yingfang Wang, Jacky Cheng, Dongqing Zhang,
Shaowen Gao, Nanshu Chen, Byoung Il Choi

GLOBALFOUNDRIES

Antoine J. Bruguier, Mu Feng, Jianhong Qiu, Stefan Hunsche, Liang Liu, Wenjin Shao

Brion Technologies

ABSTRACT

With shrinking feature sizes and error budgets in OPC models, effective pattern coverage and accurate measurement become more and more challenging. The goal of pattern selection is to maximize the efficiency of gauges used in model calibration. By optimizing sample plan for model calibration, we can reduce the metrology requirement and modeling turn-around time, without sacrificing the model accuracy and stability. With the Tachyon pattern-selection-tool, we seek to parameterize the patterns, by assessing dominant characteristics of the surroundings of the point of interest. This allows us to represent each pattern with one vector in a finite-dimensional space, and the entire patterns pool with a set of vectors. A reduced but representative set of patterns can then be automatically selected from the original full set sample data, based on certain coverage criteria. In this paper, we prove that the model built with 56% reduced wafer data could achieve comparable quality as the model built with full set data.

Keyword: OPC, model calibration, test pattern coverage, pattern selection

1. INTRODUCTION

In OPC model building process, appropriate wafer data sampling plan plays a key role. On the one hand, the empirical OPC model is calibrated with selected wafer data sets, which are supposed to represent the real product design. If the selected wafer data have insufficient coverage, the built model is likely to be unstable due to failure in interpolation or extrapolation. On the other hand, excessive data collection will not guarantee an OPC model with better accuracy and stability. The redundant gauges contribute little to a more accurate estimation of the model parameters. Moreover, the model building cycle time will be limited by the metrology loading. Instead, if we use a set with fewer gauges in calibration; we can reduce modeling turn-around time significantly. Moreover, having fewer gauges for calibration means higher measurement quality for the same SEM budget. Accordingly, it is necessary to come up with a method for data selection with optimum coverage. In this paper, we will investigate the feasibility of using Tachyon Pattern-selection-tool for data selection.

Pattern selection is a promising approach to support reliable OPC solution while controlling cost-of-ownership for smaller tech-nodes. And the reported methods for optimizing sampling plan are mainly using the image parameter analysis [1-4]. Other approach looks at how image parameters vary when the illumination conditions change [5]. However, these approaches only take into account the behavior of the gauges under varying optical conditions, and do not try to capture the resist behavior. With the Tachyon pattern selection tool, we seek to parameterize and bin the patterns, by assessing dominant characteristics of the surroundings of the point of interest. This allows us to represent

Optical Microlithography XXIV, edited by Mircea V. Dusa, Proc. of SPIE Vol. 7973,
79732K · © 2011 SPIE · CCC code: 0277-786X/11/$18 · doi: 10.1117/12.881575

each pattern with one vector in a finite-dimensional space, and the entire pattern pool with a set of orthogonal vectors. A reduced but representative set of patterns can then be automatically selected from the full set, based on certain coverage criteria. By down sampling the vectors in this pattern coverage space while keeping the coverage distribution volume and shape, smaller number of gauge patterns can take equivalent effects in calibration flow as original full gauge set. Pattern selection tool realizes a platform to optimize gauge files for better model quality and more efficient calibration flow. In this paper, we will first create a parametric reference domain to represent the real chip designs. Then the coverage of original data set could be checked by overlapping with the reference domain in vector space. Furthermore, the coverage of the hot spots of real chip and SRAM designs in vector space are verified. Finally, the pattern selection is done with the result of 56% of data points are reduced, and the comparable model quality is achieved.

2. ORTHOGONAL VECTOR SPACE

The photolithography is a complicated process that is related to a series of physical and chemical effects, including illumination and projection optics, optical interaction with photoresist, chemical effect induced by the exposure. Ideally, after the selection, the chosen patterns excite all the known physical and chemical effect, making sure that the wafer data for the test pattern can drive the model to the optimal parameter values that realize the upper-bound imposed by the formulation. The calibrated OPC model involves all the relevant parameters like sigma, NA, shape of soucemap, optical properties of layer stack, etc to accurately predict CD or EPEs. The patterns that are selected for wafer metrology and model calibration should be sensitive to one or more specific model parameters, but those with similar sensitivity characteristics to the model parameters could be dropped as the duplication of test patterns will not help improve the calibration of models. After pattern selection, the least number of patterns are selected that have high sensitivity to individual model parameters and clear distinct between the contributions from different model parameters.

In the pattern selection, each pattern may is characterized by P numbers, stored inside with a vector,

$$V_g = [S_{g1}, S_{g2}, S_{g3}, ..., S_{gP}] \tag{1}$$

the exact description of how to compute these numbers is beyond the scope of this paper but it is noted that the approach differs from [5].

Furthermore, for a pool of patterns, the sensitivity is represented with a $G \times P$ dimension matrix,

$$M_{gp} = \begin{bmatrix} S_{11} & S_{12} & \dots & S_{1P} \\ S_{21} & S_{22} & \dots & S_{2P} \\ \dots & \dots & \dots & \dots \\ S_{G1} & S_{G2} & \dots & S_{GP} \end{bmatrix} \tag{2}$$

where P is the dimension of the space, G is the number of total pattern gauges.

Since the each pattern is characterized by a P dimensional vector, visualization is difficult. We can do a PCA (Principal Component Analysis, also known as SVD for Singular Value Decomposition) on the matrix M_{gp}. The principal components of the matrix are the directions (orthogonal to each other) in the P-dimensional space that capture most variations. Thus the first principal component account for as much as the variability as possible; each succeeding component accounts for as much as the remaining variability as possible. Using this approach, each pattern can be approximated by its coordinates along three directions *(U-001, U-002, ..., U-00N)*, and the whole patterns pool can be

represented inside an orthogonal vector space. It is noted that this transformation is not necessary for the pattern selection to function, but is helpful for visualization. The following investigation on parametric reference domain and pattern selection is all based on this vector space, where we keep the first 3 principal components with most energy.

3. REFERENCE PARAMETRIC DOMAIN

3.1 Reference Domain study

This part is to study a parametric reference domain through the analysis of orthogonal vector space. Before doing the pattern selection on current full gauge set, we need build a reference domain that cover the real chip design. According to ref. 1, generalized pattern shapes for 1D and 2D respectively are employed to approximate all the product layouts. However, this method is not restricted to certain device layouts. The Tachyon pattern selection tool can function with any pattern shape. The representing patterns are put into four categories, 1D-line, 1D-space, 2D-line, 2D-space. The 1D line patterns have three geometrical sizes *w0*, *w1* and *s0*, while the 2D patterns have five geometrical sizes *w0, h0, s0, w1, h1*. By varying the parameter sizes, a big set of test pattern groups are generated. With a constant threshold model and pattern-selection-tool, the test patterns are projected into the high dimension vectors space, which are regarded as our reference domain.

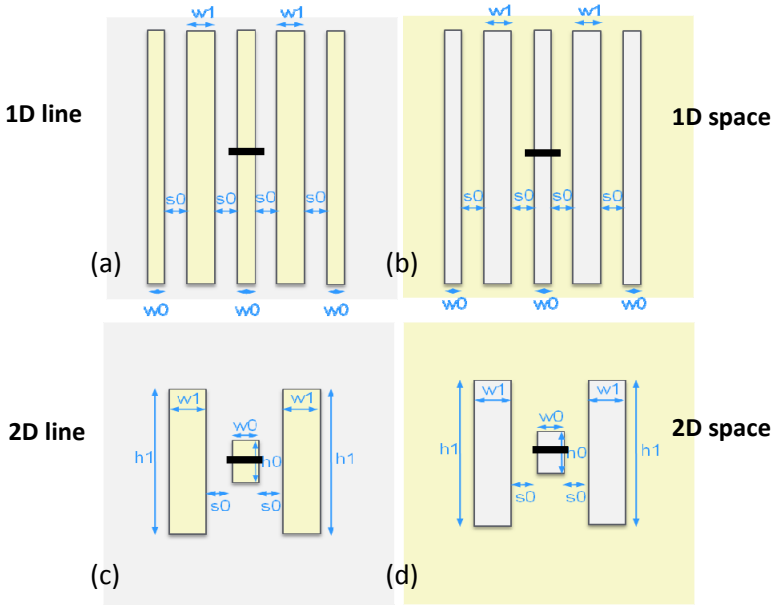

Figure 1. 1D line reference domain (top left) and space domain (top right) with varying *w0*, *w1* and *s0*, and 2D line reference domain (bottom left) and space domain (bottom right) with varying *w0*, *h0, s0, w1* and *h1*.

For 1D patterns, it is easy to relate the generalized pattern to usual OPC test pattern types, such as iso, pitch, iso-pad etc. While *s0* is big enough, it will be iso pattern; and we get pitch if *w0* equals *s0*. As for iso-pad, the *w1* should be big size. Fig. 2 shows the distribution of first three principal components of vectors within 1D line reference domain, which represent the most energy, and the distributions of rest components of vectors are less dominant so that not shown here. The red points in fig.2 (a)-(d) are taken at *w1* sizes of 1200nm, 800nm, 400nm and 100nm respectively. For example, in Fig 2(a), only those patterns with w1=1200nm are highlighted in red, whereas the patterns with other widths are in blue. It is found that *s0* and *w1* is strongly related to vector *U-001* and *U-002*, and the influence of *w0* is more *U-003*

dependent. It should be noted that the pattern selection picks up these trends without any knowledge of the pattern geometry. In other words, we do not need to tell the algorithm which patterns are 1D line, 1D space, or other; the algorithm recovers these trends on its own. The distribution of points in vector spaces is restricted to a dense area while *h0* is 1200nm and 800nm respectively, according to Fig. 2(a) and 2(b), whereas the points scatters to a bigger region in Fig. (c) and (d) while *w1* decrease further. The *w0*'s impact is stronger with the decreases of *w1*, meaning that the effect of *w0* is secondary compared with *s0* while *w1* is big. But when *w1* is smaller, *w0*'s effect is increasing. Such findings may contribute to our test pattern split designs. For example, while designing iso-pad, we may need few *w0* splits but much more space splits. In contrast, more *w0* splits should be involved when we are dealing with the small width through pitches.

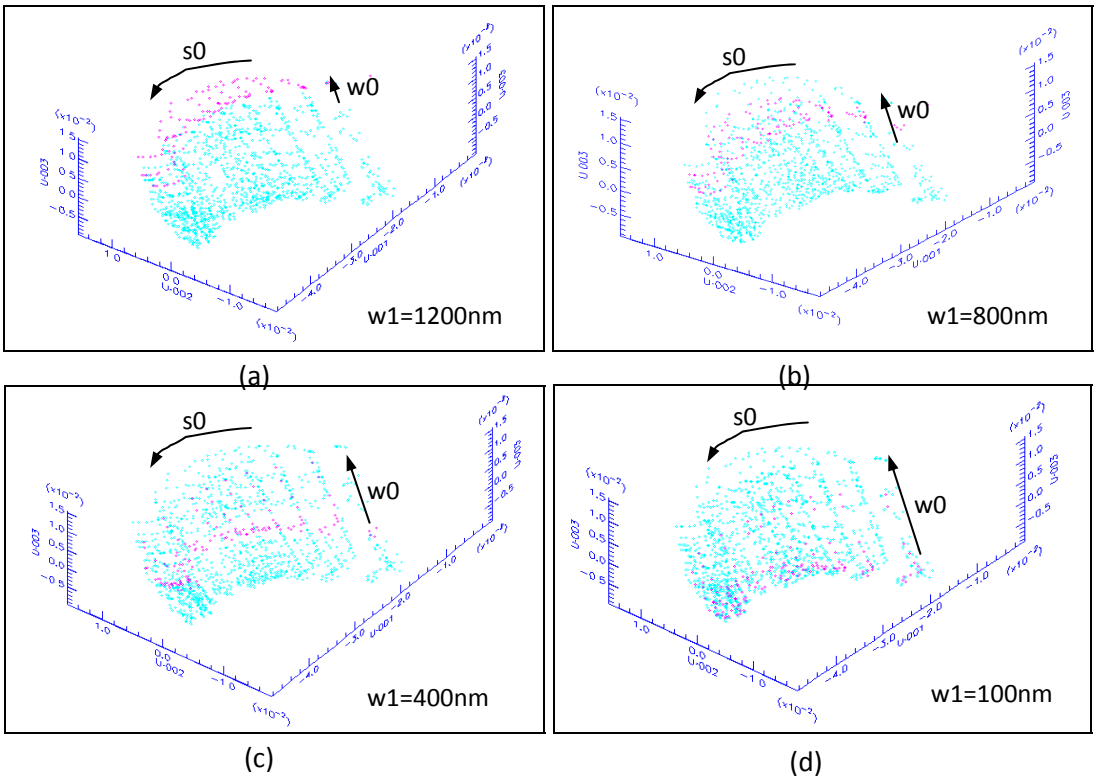

Figure 2. 1D parametric reference domain. Study the impacts of 1D patterns' *w0*, *s0* on vector space with different *w1* values of 1200nm, 800nm, 400nm, 100nm respectively. The points highlighted in red represent the different *w1* in fig. (a) – (d). Only first three principal components (*U-001, U-002, U-003*) are displayed to construct a 3D space.

For 2D patterns, similarly we can generate usual test pattern by varying the values of five parameters *w0, h0, s0, w1, h1*, such as line-end, T-junction, broken-H, island, short-bar etc. In order to simplify the analysis, we first fix *w1* and *h1* at 1000nm and 3000nm respectively. Fig. 3 shows the dependence on *w0*, *h0*, *s0* only, and the points highlighted in red correspond to *h0 of* 100nm, 150nm, 200nm, 300nm respectively in (a) – (d). It is obviously that *s0* and *w0* are the two key parameters affecting globally on the distribution of vector components. And the increase of *h0* will lead to the scattering points from outer right to left inner space. Furthermore, we tested with different *w1* and *h1* sizes, finding that they only affected locally, and the change of *w1* or *h1* does not change the shape of the distributions within vector space. In Fig. 4, *w1* is fixed at 1000nm; the (a) – (d) display distribution with varying *w0*, *h0*, *s0* at *h1=1000nm*, *300nm*, *200nm*, *100nm* respectively.

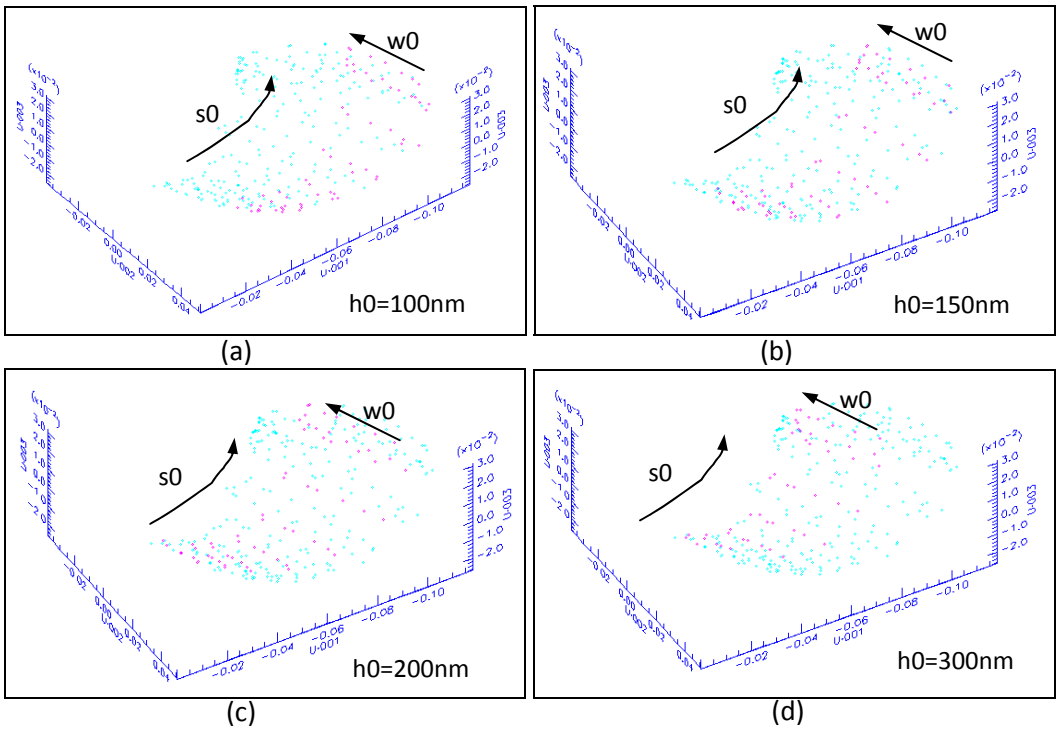

Figure 3. 2D parametric reference domain. Study of the characteristics the dependence on geometric parameter *w0*, *h0* and *s0*, while *w1*=1000nm, *h1*=3000nm. In (a) – (d), the points highlighted in red represents the points with different *h0* sizes of 100nm, 150nm, 200nm and 300nm respectively.

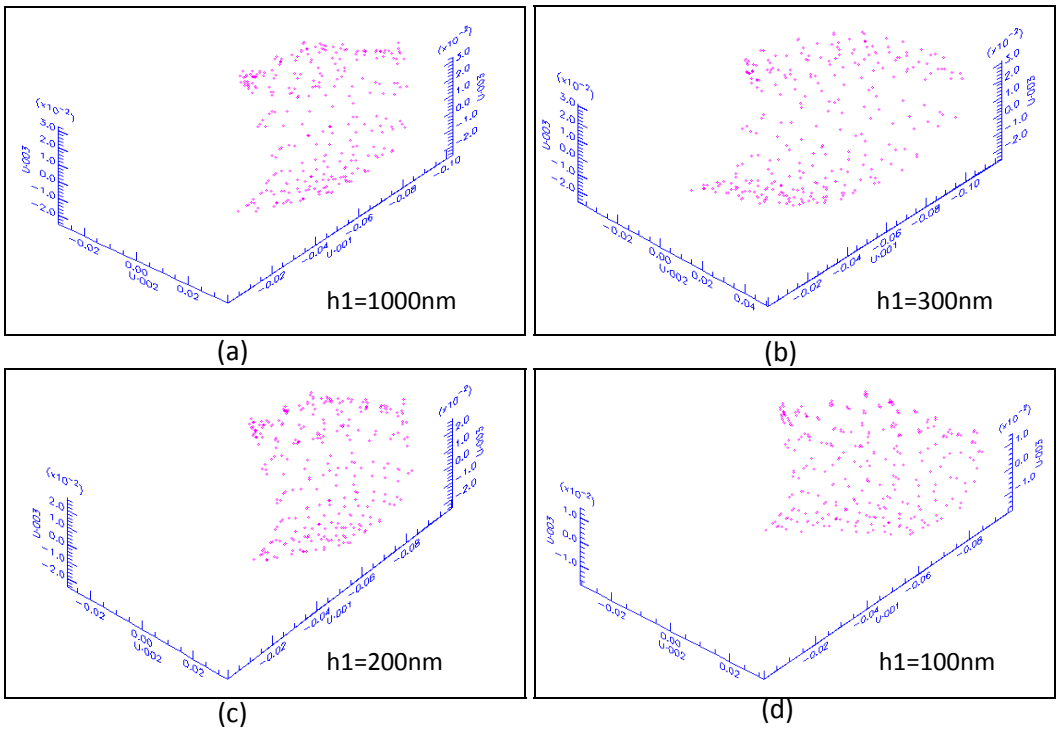

Figure 4. 2D parametric reference domain. Study of parametric domain with respect to the varying geometric parameter *w0*, *s0*, *h1*, and *w1*=1000nm. Figure (a) – (d) represents *h1* = 1000nm, 300nm, 200nm, 100nm respectively.

3.2 Original sampling plan coverage

By overlapping the projected vectors spaces of original full sampling plan (before pattern selection) and reference domain, we could check whether the current data sampling is sufficient or not. Fig. 5(a) and (b) show the overlapping result of current 1D line patterns with reference domain from different perspective view. It is found that overall current sampling could represent the reference domain well, but with some redundancies in certain area. Fig 6(a) and (b) provide the 1D space sampling data coverage condition in different perspective. Although a large part of areas are not included, we have confirmed that current sampling plan is enough to represent the typical chip layout designs, for the reference domain usually occupies wider region than those real chips.

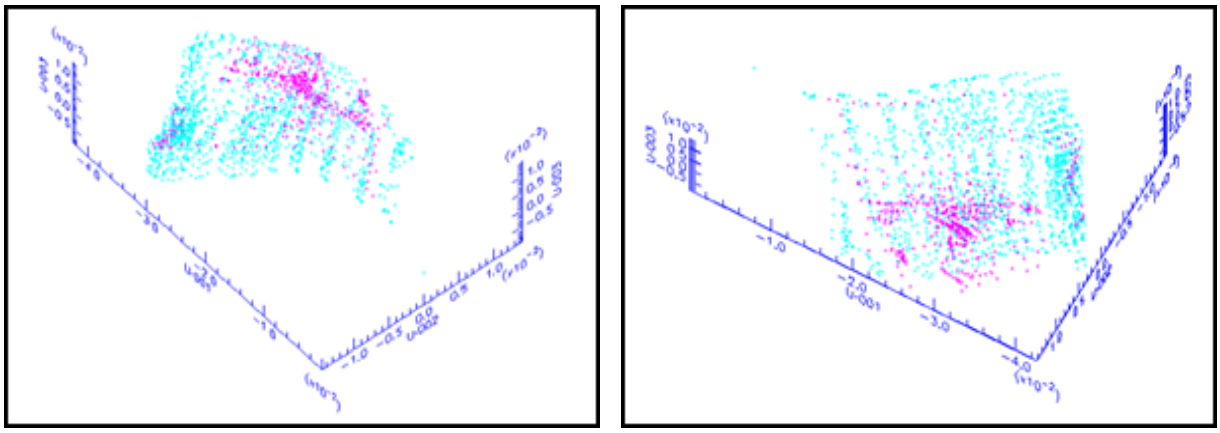

(a) (b)

Figure 5. Original full-gauge (before selection) 1D line sampling projection (red) overlapping with representing domain (blue) in parameter space. (a) and (b) display from different perspective.

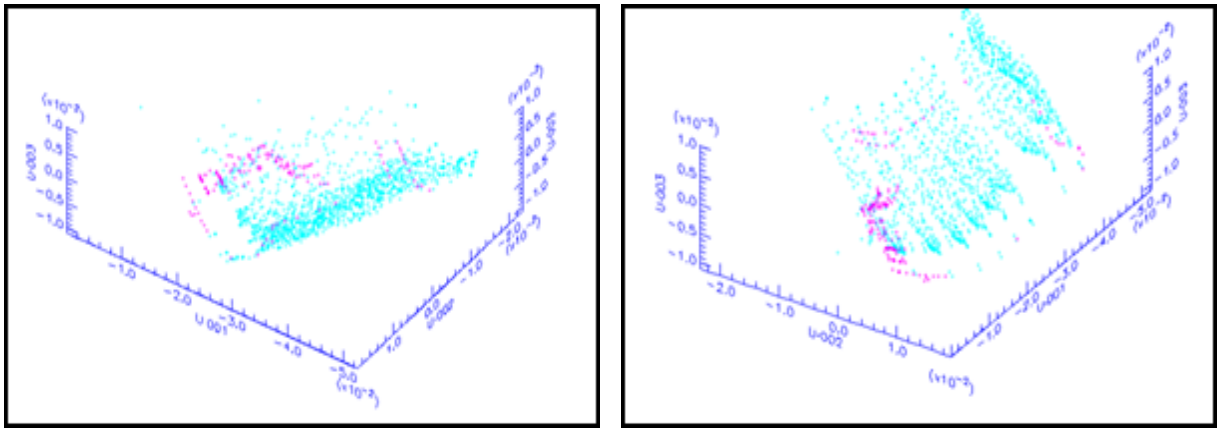

(a) (b)

Figure 6. Original full-gauge (before selection) 1D space sampling projection (red) overlap with representing domain (blue) in parameter space.

3.3 Hotspots and SRAM coverage

Additionally, we will check whether the current sampling plan covers the full-chip hot spots and SRAM layouts. Fig. 7(a) and (b) show the coverage results viewed from two different perspectives. In the figure, those points highlighted in red are representing hotspots and SRAM points extracted from production chip, while the blue points are original sampling points. According to Fig. 7(a), line patterns and space patterns are separately distributed within the vector space. It is observed that overall SRAM and hotspots patterns are covered by our current sampling plan well, except for small number of SRAM space patterns and 2D Hotspots. Specifically, some SRAM space patterns with shapes similar to dense short bar patterns are not totally covered, as it is shown in Fig. 7(b). And the uncovered hotspots are mainly two type, one is close to T-junction shape with thick-width side attacking bar measuring line (pinch concern), and the other is similar to test pattern broken-H shape measuring space (bridging concern). Accordingly, we include some corresponding test patterns with similar shapes and sizes in our OPC model verification data set for post model calibration check. This will help improve the stability of final OPC model.

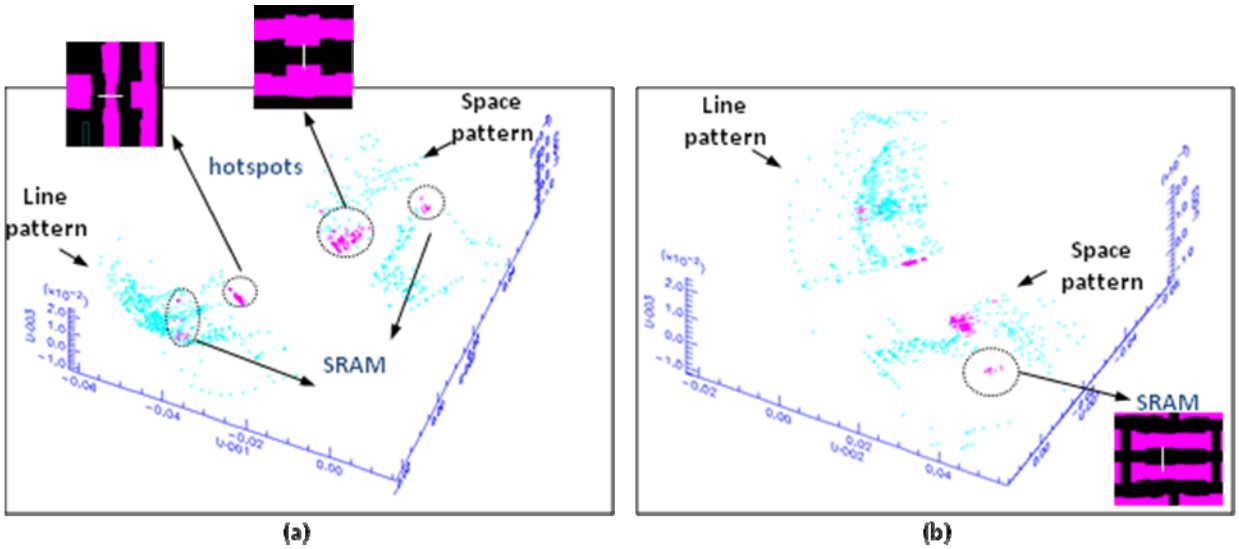

Figure 7 (a) Overlap current sampling data points with full-chip ORC hot spots in principal components vector space. The red points represent the SRAM and hotspots, while the blue points correspond to full-set sample points. (b) shows the same result but is viewed from another perspective, it can be observed that the SRAM space pattern is not well covered and we remedy this problem by adding similar test pattern to the model verification data set.

4 PATTERN SELECTIONS

Fig. 8 shows the schematics of the procedures of pattern selection, which is enabled by Tachyon's pattern-selection-tool. First we need create a purely optical model (constant threshold) based on the process conditions and using only an anchor gauge. Subsequently, by setting a target gauge number, the pattern selection is done with original full sample gauge and base model. It is noted that no wafer data is required in the pattern selection, and the tool is restricted to data selection at nominal process conditions. But it may help build a better base model if the users have some preliminary process window wafer data at the stage of pattern-selection. After the pattern selection, we get a gauge with reduced number of points, which we call sub-set gauge here, compared with the original full-set gauge. Subsequently, a model can be calibrated with this reduced sub-set gauge (include wafer data). In addition, we will also build a model based on full-set gauge for comparison.

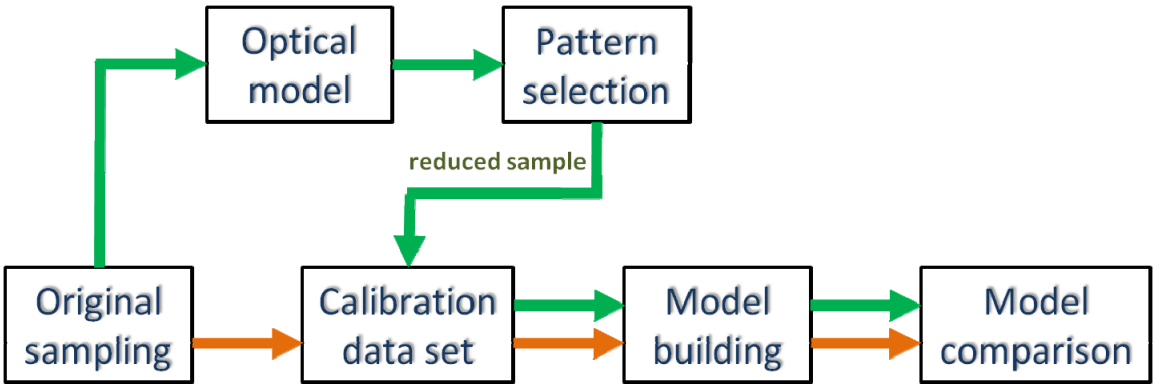

Figure 8 Schematic of pattern selection procedures. The orange flow is normal model calibration flow, whereas the green flow includes the pattern selection step before model building.

In order to understand the relationship between model quality and pattern selection numbers, we performed the pattern selection four times by reducing the gauges points by 34%, 45%, 56% and 67% respectively. Based on these sub-set gauges with wafer data, four models are calibrated, and fig. 9 provides the comparison of model error RMS for the totally five models. Although only sub-set data are used in model calibration, the overall error RMS displayed is based on the full-gauge data for comparison. Furthermore, we go into the details of the fitting result for each pattern groups, finding that the model built with the subset data of 56% reduction could satisfy our spec. Fig. 10 shows the pattern selection result in principal components vector space with pattern-selection-tool. The red points represent those selected gauges, whereas the blue points are regarded as redundancy and removed from calibration gauge. In order to further compare the model quality of model built with original full set data and selected sub-set data, we classify the patterns into different pattern groups. Fig. 11(a) provides the comparison of percentage of pattern group numbers between original full-set and sub-set gauges, and group model error RMS for each pattern group are shown in Fig.11(b). It is noted that the relative distribution of the patterns is changed after the selection. This is a desirable feature of the selection algorithm: it removes patterns more aggressively in the groups which are overrepresented. Finally, the full-chip contour matching is done with the two models and the matching histogram is shown in Fig.12.

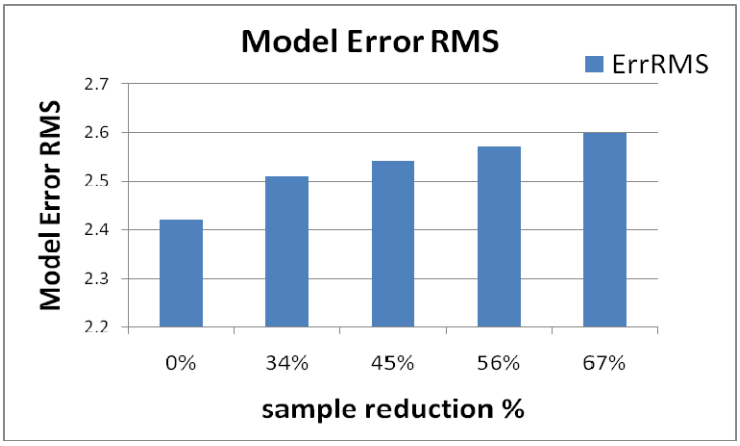

Figure 9 Model Error RMS versus sample reduction percentage.

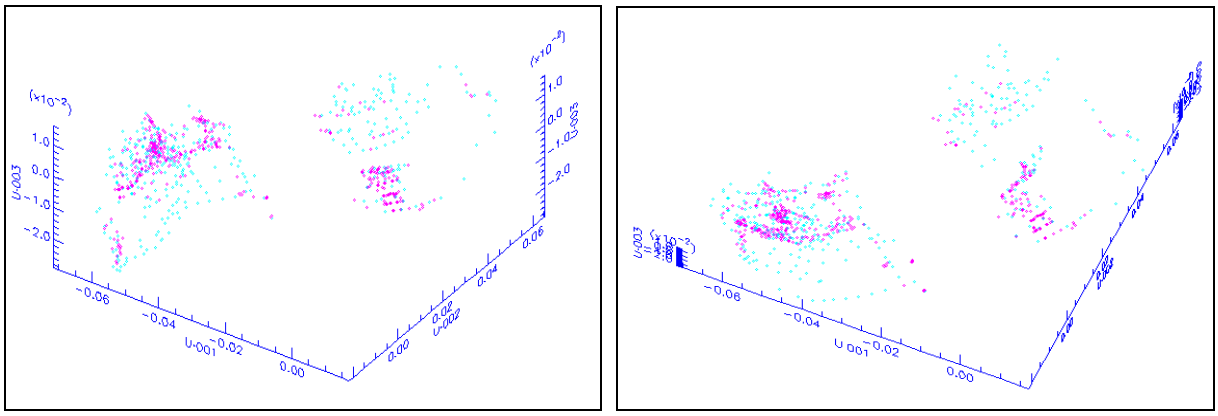

Figure 10 Pattern selections (56% points dropped) in parameter space. Red points represent 44% selected gauges whereas green points are dropped.

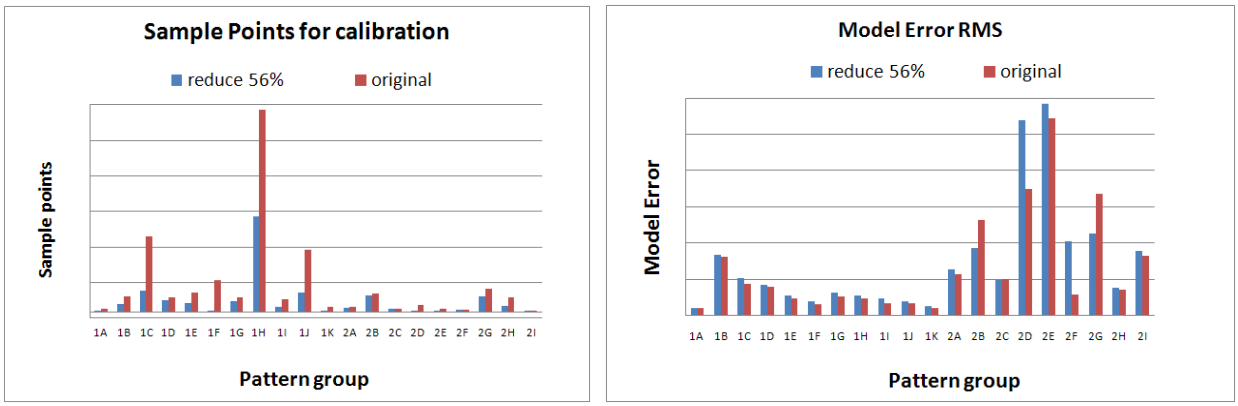

Figure 11. Model performance comparison by pattern groups between models built with original full gauge and with 56% reduced pattern gauges. 1A – 1K are 1D pattern groups, and 2A – 2I are 2D pattern groups.

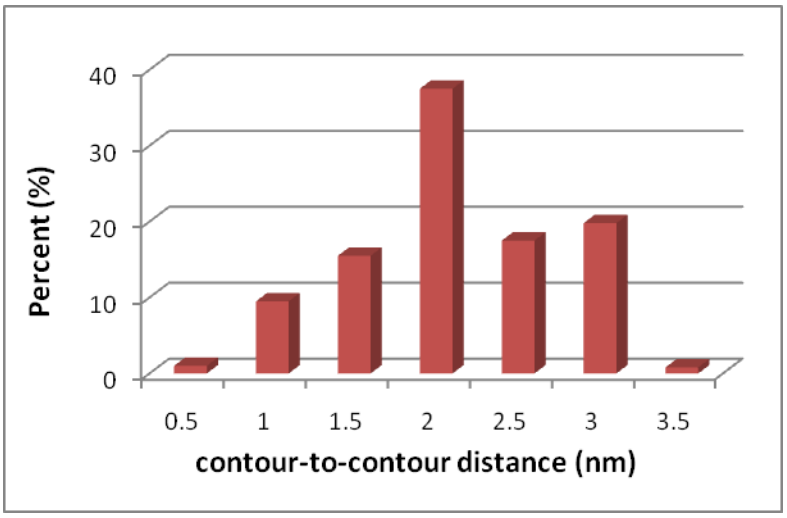

Figure 12. Distribution of full-chip contour-to-contour distance

5 SUMMARY

In this paper, we have studied a series of topics relevant to OPC model test pattern based on the vector space of Tachyon pattern-selection-tool, including parametric reference domain, coverage check, and pattern selection. The generalized 1D and 2D pattern shapes are designed to approximate all the product layouts and the impact of geometric parameters on the distribution in vector space are investigated. The coverage of original data sample is checked through two methods, one is by the parametric reference domain, and the other is overlapping with hotspots and SRAM patterns. The pattern selection flow is introduced and it is demonstrated that the model built with 56% reduce sub-set gauges could achieve comparable quality as those built with full set gauges. The comparisons include overall model error RMS, pattern group error RMS, and full-chip contour comparison.

References

[1] A.Khoh, S.F. Quek, Y.M.Foong, J. Cheng, B.I. Choi, “Maximizing test pattern coverage for OPC model build ”, Proc. SPIE 6154, 615437 (2006)

[2] K. Patterson, Y. Trouiller, K. Lucas et al., “Improving model-based OPC performance for the 65nm node through calibration set optimization”, Proc. SPIE 5756, 294 (2006)

[3] J. Oberschmidt, A. Abdo, T. Desouky, M. Iman et al., “Automation of sample plan creation for process model calibration”, Proc. SPIE 7640, 76401G (2010)

[4] A. Abdo, R. Viswanathan, “The feasibility of using parameters for test pattern selection during OPC model calibration”, Proc. SPIE 7640, 76401E (2010)

[5] Y. Cao, W.J. Shao, J. Ye, R. J. G. Goossens, “Pattern selection for lithographic model calibration”, U.S. Patent 2010/0122225 A1, application on May 13 (2010)